

# Modeling Action Potentials of Body Wall Muscles in *C. elegans*: A Biologically Founded Computational Approach

Callen Johnson and Roger Mailler

Computational Neuroscience and Adaptive Systems Laboratory, The University of Tulsa  
Tulsa, OK, 74104, USA  
callen-johnson@utulsa.edu

## Abstract

The nematode *Caenorhabditis elegans* (*C. elegans*) is a model organism that despite years of intensive effort still presents researchers with numerous mysteries to explore. One of the most intriguing unanswered questions involves the function of the neural circuitry used for locomotion. There are several computational models that attempt to explain how this circuit works, but with a lack of physiological information, they rely on parameters that were derived using optimization techniques.

Recent advances in electrophysiological and optogenetics have finally allowed researchers to directly measure these parameters and, not surprisingly, show that the values produced by the optimization algorithms significantly depart from reality. This work takes a first step in resolving this disparity by presenting a novel computational model of a *C. elegans* body wall muscle cell that is solely based on actual electrophysiological data. Unlike current models that create graded potentials, this model produces all-or-nothing action potentials, which matches *in vivo* measurements.

**keywords:** *C. elegans*, EGL-19, muscle, SHK-1

## 1 Introduction

### 1.1 Towards a Model For Locomotion

Modeling of a fully functional central nervous system has made significant advances due to research conducted on the model organism *C. elegans*. This nematode has a seemingly manageable nervous system, with 302 neurons and 95 body muscle cells [21] that, along with its small size and reproducibility of its nervous system, has already provided researchers with an almost complete map of synaptic connectivity in the adult hermaphrodite [20]. The fact that this connectivity map is incomplete is evident in the lack of a thorough understanding of how the *C. elegans* performs even the basic task of locomotion.

Electrophysiological studies on the neurons and their interconnections seems to be the most obvious way to get direct measurements; however, this method suffers its own limitations. Direct recordings of the electrical activity in *C. elegans* requires access to the neuron under investigation. This implies penetrating the cuticle into the hydrostatically pressurized pseudocoelom *pops* the worm. This damages the internal structures and makes further measurements pointless.

Without a means of obtaining the information necessary for completing a model of the *C. elegans* locomotion, attempts have been made to simulate its movement. Using forward locomotion as its basis, Neibur and Erdös were able to produce a simulation in which they showed that the use of stretch receptors could propagate locomotion waves [17]. In this simulation, Neibur and Erdös used a sine wave function to drive the locomotion, ignoring the actual circuitry known to be used by the worm itself. Later works by Bryden [3] and Karbowski [10] furthered this view by developing biologically inspired neural network simulators which produce forward locomotion. While Neibur and Erdös left out low-level details pertaining to the functioning of cells, the model proposed by Bryden relies heavily on filling in the missing pieces with parameters made using an evolutionary fitting algorithm. The results of this model led to invalid conclusions that focused on graded potentials in body wall muscles, as reported by Jospin *et al.* [8], and the belief that gap junctions connecting muscle cells have no role with action potentials in body wall muscles, which has been shown to be incorrect (see Liu *et al.* [12]).

Even though these models produce motion, they fail to demonstrate what *is* actually happening. The reasons for this are that these simulations make use of very abstract representations of the *C. elegans* body, modeling it uniformly in two dimensions, which fails to replicate much of the basic physics of locomotion (such as weight distribution, contact friction, and non-uniform positioning of muscle tissue used in generating movement). Additionally, the neural networks that are used in driving the simulations are extremely simplified

models of the *in vivo* nervous system. Examples of this are Neibur and Erdős’ neglect of AS-type neurons and the previously mentioned use of parameters that were the result of machine learning techniques to reproduce the worm’s gait. Furthermore, there may be any number of different settings in the models that would actually lead to the correct behavior, but lay outside of what is physically possible. Even with the generation of motion, these models cannot explain nor replicate the robust and adaptable behavior of the worm itself.

Recently, techniques have been developed that allow researchers to probe individual muscle cells (and pairs of cells), motor neurons and interneurons, taking measurements without causing extensive damage to the internal structure of the worm. In addition, techniques that rely on encoding calcium indicators and optically activated channels in the worms have been developed. These techniques have allowed for many new advances toward completing the map of the *C. elegans* neurocircuitry [14] [13] [15] [12]. These new developments have seen that not only do the muscle cells generate all-or-none action potentials [14], but also that the gap junctions between the muscle cells actually synchronize them along with  $\text{Ca}^{2+}$  transients [13], indicating that the results of the previous models simulating locomotion are removed from what is actually happening.

In this report we present a novel computational model of a *C. elegans* body wall muscle cell that is based solely on the actual electrophysiological data. We demonstrate here that all-or-none action potentials resembling *in vivo* measurements are produced by our model.

## 1.2 Background

In the adult hermaphrodite *C. elegans* there are 95 body muscle cells. The primary body wall muscles are distributed in four rows made from 23 to 24 muscle cells in an interleaving pattern [4]. Near the anterior of the worm the cells are overlapping pairs with the level of overlapping decreasing toward the posterior. This cell structure restricts the worm’s movement to dorsal and ventral bending as a wave propagates forward (or backward) along the worm’s body. This generates a sinusoidal pattern of locomotion.

Studies have shown that these body wall muscle cells generate all-or-none action potentials [14] that are interestingly caused by something other than  $\text{Na}^+$  channels. In fact, there are no known voltage-gated  $\text{Na}^+$  channels encoded in *C. elegans* [2]. Instead, the action potentials are dictated by  $\text{Ca}^{2+}$  and generated by the intake of  $\text{Ca}^{2+}$  into the muscle cell through an L-type voltage-gated calcium channel (VGCC), EGL-19, with some possible contribution from another VGCC known as

CCA-1 [19] (T-type calcium channel). Research shows that the EGL-19 channel is voltage activated while its inactivation is based on both voltage and  $\text{Ca}^{2+}$  [11]. The concentration intake of  $\text{Ca}^{2+}$  triggers a release of stores of more  $\text{Ca}^{2+}$  from the sarcoplasmic reticulum [14]. Calcium is responsible for the functioning of the muscle cell’s actin and myosin, making the muscles contract.

The ion channels responsible for the action potential upstroke are different from those of the cell’s repolarization [14]. There are three outward current carriers in the cell: the SHK-1, SHL-1 and SLO-2 ion channels [18]. The Kv4 channel SHL-1 [5] only has a small contribution while SHK-1, a Kv4 delayed-rectifier and voltage-gated potassium channel, works in conjunction with SLO-2 to control how fast the cell repolarizes, the depth of the afterhyperpolarization, and the firing pattern of the action potentials [14]. The SLO-2 channel has been called the predominant outward current carrier [18] [5] and requires the EGL-19 channel’s intake of calcium in order to activate (being that it is  $\text{Ca}^{2+}$ - and  $\text{Cl}^-$ -gated).

## 2 Model

### 2.1 Development of the Simulated EGL-19 Channel

Our computational model is based on the Hodgkin and Huxley model [7] considering specific ion channels and their steady and nonsteady-state activation (and inactivation) gates as they affect a channel’s conductance. Producing functions to describe the steady and nonsteady-state dynamics of the EGL-19 channel required the consideration of the peak and end pulse currents from previous reports [11] [14]. It is known that the EGL-19 has an activation and an inactivation gating parameter, here defined as  $m$  and  $h$ , respectively. The peak current signified the behavior of the channel’s activation gating parameter,  $m$ , whereas the end pulse current accounted for both the activation and the inactivation,  $h$ , dynamics. The *in situ* patch-clamp data used to derive the functions employed by our computational model came from previously published findings [11] [8] where I-V relationships were given.

In order to reproduce these I-V curves we considered the calcium current that flows through the EGL-19 channel and modeled it using an equation that accounts for the channel’s conductance,  $g_{Ca}$ , with the form

$$I_{Ca} = g_{Ca}(V - E_{Ca}) \quad (1)$$

where  $E_{Ca}$  is the reversal potential for the channel and has a value of 46 mV [14], while  $V$  is the model

muscle cell's potential. The calcium conductance is determined based on values of the channel's activation and inactivation parameters by:

$$g_{Ca} = \bar{g}_{Ca} m^2 h \quad (2)$$

The steady-state value of this conductance  $\bar{g}_{Ca}$  is given as 284 S/F [11] (The units S/F represent normalized conductance in siemens per farad). The function for activation,  $m$ , was tested using a custom built patch-clamp simulator in MATLAB [16] with its embedded fourth-order Runge-Kutta ordinary differential equation solver and was validated by comparing the activation with those recorded from the actual *C. elegans* worm [14] [11] [8] [9]. The activation gate is updated throughout the computational simulation of the model cell using a scheme adopted from Hodgkin and Huxley [7]:

$$\tau_x \frac{dx}{dt} = -[x - x_\infty] \quad (3)$$

In equation 3 the symbol  $x$  is used as a simple placeholder in which the appropriate notation with respect to the ion in question can be substituted in, as will be done for the SHK-1 potassium channel.  $\tau$  is the time constant for the ion channel which is 1 ms for activation and 7 ms for inactivation [6]. The steady-state value of activation, notated as  $x_\infty$ , is characterized by Boltzmann kinetics using the form

$$x_\infty = \frac{1}{1 + \exp\left[\frac{-(V - E_{0.5})}{k}\right]} \quad (4)$$

where  $E_{0.5}$  is the potential for half activation and has a value of 6.7 mV [11] and  $k$  is the steepness factor and is 4.5 mV [11].

The simulated patch-clamp program was written using a common technique where currents were measured after applying a steady voltage for a duration of time, allowing it to stabilize, as a guideline. The curves were then fitted using the equation

$$I = g(V - E) / (1 + \exp\left[\frac{-(V - E_{0.5})}{k}\right]) \quad (5)$$

The voltage dependence of the normalized conductances were then determined by dividing the above equation by  $g(V - E)$  then fitted using the above described Boltzmann equation. Since the data describing the peak and end pulse currents were implicitly given in the report by Lainé *et al.* [11] and the values were explicitly stated, the above equations were trivial to construct. The result of these equations is shown in the graph of Figure 1 and can be compared with those shown by Lainé *et al.* [11].

EGL-19 Peak and End Currents

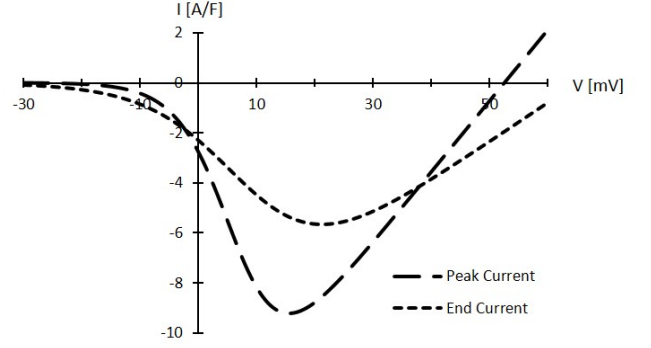


Figure 1: The peak and end currents as described by Lainé *et al.*. This patch-clamp measured data represents the biological basis of which the simulated EGL-19 channel was founded. These curves were made using the data from previously reported findings in functions applied to the computational model (The Y-axis is normalized current in units of amps per farad, or A/F).

Isolating the data for the channel's activation yields the peak and end percent activation of the EGL-19 channel as voltage is increased, shown in Figure 2.

EGL-19 Peak and End Activation

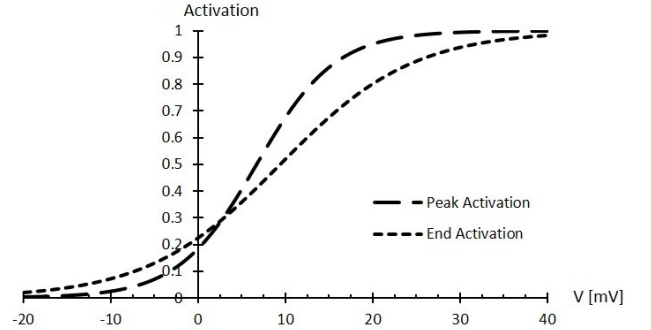


Figure 2: The peak and end activation dynamics of the simulated EGL-19 channel. The Y-axis in this figure represents the conductance channel's activation percentage, where 1.0 is 100%.

The calcium channel's inactivation parameter,  $h$ , was modeled using a Gaussian function which was described by Jospin, *et al.* [8] as having a bell-shape. Using this description, the Gaussian function to describe the steady-state is

$$h = 1 - A \exp\left[\frac{-(V - B)^2}{2C}\right] \quad (6)$$

Using the general form of the Gaussian equation  $A$  is the amplitude of the inactivation curve and is 0.516,  $B$  describes the height with a value of 13.508 mV and  $C$  is its standard deviation of 19.48 mV. These values and the Gaussian behavior of the inactivation were described by Jospin *et al.* [8]. This inactivation gating function was more difficult to recreate since the peak current was less than the end current in many places in the data (see Figure 1), and its behavior has been mentioned [6] [11] [8] but no sufficient data has been reported for *C. elegans*.

The form of this function is due to the best description of the EGL-19 inactivation gate's behavior thus far [8]. Many function fits were tried on the data provided in the report, including a polynomial up to five degrees and a Boltzmann. Based on the reported bell shape description, it was decided that a Gaussian would be used. It can be seen in the graph of Figure 3 that the Gaussian fit, based on biological data, provides the best fit when compared to the literature.

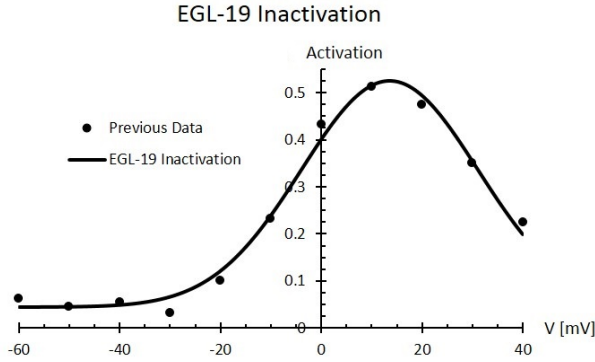


Figure 3: The inactivation parameter of the EGL-19 channel is described using a Gaussian equation.

The curve fitting that was performed in order to compare to previously published results was done using Mathematica [1].

## 2.2 Development of the Simulated SHK-1 Channel

Using the same methodology as described above for the EGL-19 channel, the dominate outward current potassium channel, SHK-1, functions were modeled using the information provided by Jospin *et al.* [9] for the peak current. The SHK-1's current equation has the familiar form

$$I_K = g_K(V - E_K) \quad (7)$$

where its reversal potential,  $E_K$ , is 70 mV [18]. The

conductance is described as

$$g_K = \bar{g}_K n^4 \quad (8)$$

where the steady-state conductance  $\bar{g}_K$  is 564 S/F [14]. The activation gating parameter  $n$  dictates the activation of the channel and was modeled using the same technique as with the EGL-19 activation gate,  $m$ , using peak current data. End pulse data was not included when considering steady-state information as the channel does not have an inactivation gate. The equations used to derive the simulated activation are the same as in equations 3, 4 and 5, where the time constant, potential at half activation and steepness are 190 ms, 1.237 mV [14] and 6.859 mV [14], respectively.

The graph in Figure 4 shows the peak current for the activation of SHK-1, and, using these parameters, the equations describing the behavior of the SHK-1 activation were validated again by the simulated patch-clamp experiment in the same manner as with the EGL-19 activation gate. The graph in Figure 5 shows the comparison between the model's SHK-1 activation and that of the *in situ C. elegans* recordings reported by Liu *et al.* [14].

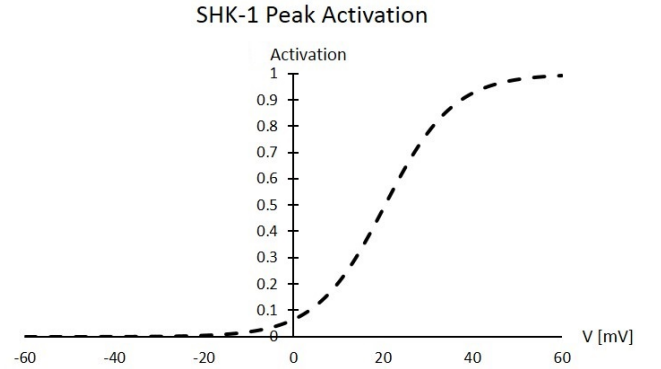


Figure 4: The peak activation for the SHK-1 channel using functions derived from previously reported parameters found in both Liu *et al.* [14] and Jospin *et al.* [9].

## 2.3 Leakage Current

Since the present version of the model was assembled to test whether or not it was possible to produce action potentials by employing data solely measured from the living worm, a leakage channel was required to mask the effects of the additional channels that are not yet accounted for. Then leakage current is described using

$$I_L = g_L(V - E_L) \quad (9)$$

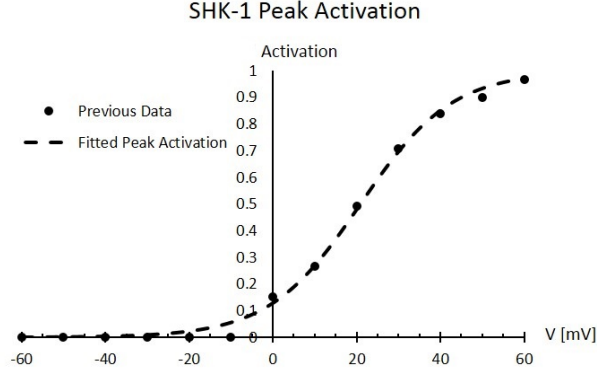


Figure 5: The activation for the SHK-1 channel is described using Boltzmann kinetics in a simulated patch-clamp experiment, matching biological data previously reported.

where the leakage conductance is given as  $g_L = 17.2$  S/F [14], and the reversal potential is -13 mV [14].

## 2.4 Conductance-Based Modeling of Body Wall Muscles

Using the above currents,  $I_{Ca}$ ,  $I_K$  and  $I_L$ , the model muscle cell simulation was performed using a conductance-based design, following in the likeness of the Hodgkin and Huxley model [7]. The muscle cell's potential is determined using

$$C_m \frac{dV}{dt} = I_{ext} - I_L - (I_{Ca} + I_K) \quad (10)$$

where  $I_{ext}$  is externally applied current in nA and  $C_m$  is the membrane capacitance. Since the conductances used in the model are normalized, the capacitance is not taken into account. This potential was updated through simulated time in ms in MATLAB [16] using its fourth-order Runge-Kutta function, as was done in the patch-clamp simulator.

## 3 Results

Using the functions derived from biological data, the computational conductance-based model results in action potentials in the model muscle cell, seen in Figure 6. By applying an external current of  $1 \mu A$  the model cell demonstrated spiking behavior. It is important to note here that these action potentials were a direct result of using only values reported from *in situ* experiments for the calcium and fast potassium currents, not the result of evolutionary fitting algorithms. Figure 7 shows a closer view of the action potentials elicited by the model in 400 ms of

simulated time along with the behavior of the activation and inactivation gating dynamics.

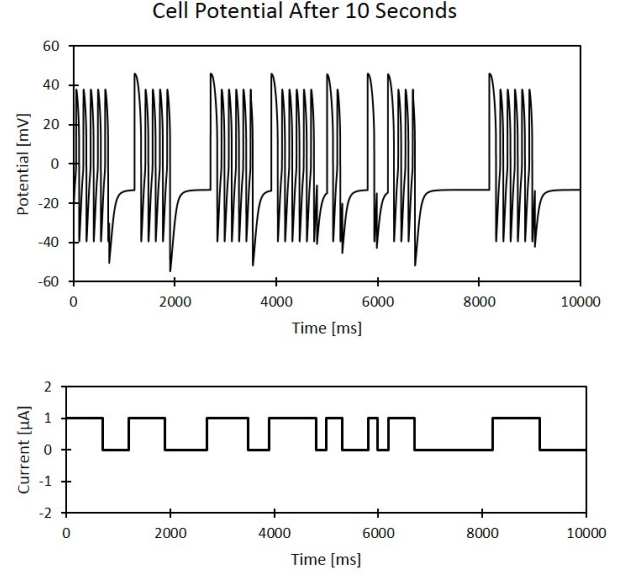


Figure 6: Action potentials in the model muscle cell were produced using only functions and parameters obtained from electrophysiological data that has already been published, following a  $1 \mu A$  applied current pulse.

The action potentials shown in this figure have resemblance to those reported by Liu *et al.* [14] for the *slo-2* mutant. This is seen in the fast upswing of the depolarization, and similarity in the values for the cell's resting potential (-17.2 mV), the action potential amplitude (54.8 mV), width in ms (56.9 ms), and the depth of the afterhyperpolarization (16.8 mV).

The lower graph in Figure 7 demonstrates the fast activation of the EGL-19 channel coinciding with the drop in its inactivation parameter which brings the action potential to its peak value. After this peak potential is reached, the SHK-1 channel's activation begins to rise, working in tandem with the EGL-19 inactivation gate in order to repolarize the model muscle cell.

## 4 Discussion

A successful recreation the EGL-19 and SHK-1 ion channels that are known to exist in the body wall muscle cells of the *C. elegans* [8] [9] has been demonstrated. These channels are also known to be major contributors to the generation of action potentials [14]. The previous computational models attempting to recreate the action potentials employed a method allowing only

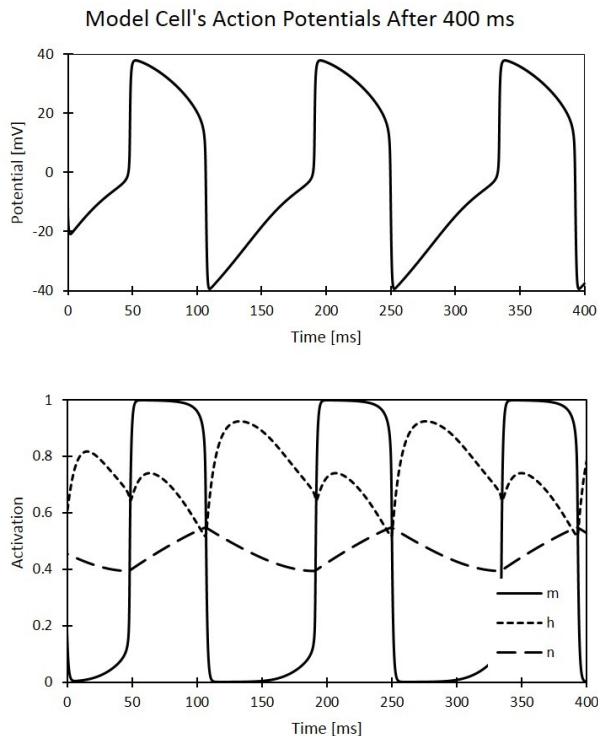


Figure 7: A close-up view of the action potentials produced by the model (top) along with a graphical description of the behavior of activation gating parameters  $m$ ,  $n$  and inactivation parameter,  $h$  (below).

some of the parameters required to come from actual measurements from the worm while the rest were fitted by an evolutionary fitting algorithm [3]. The result was a complete model of the body wall muscle cell that incorrectly produced graded potentials and played down the significance of the gap junctions connecting them.

Here it is shown that by considering only the two primary channels required for action potential generation in *C. elegans* and their biologically measured parameters, we can produce action potentials that resemble those actually observed in the worm. Consider for comparison the *slo-2* mutant, as this mutant lacks the expression for the SLO-2 channel in its genetic code, leaving the primary channels as EGL-19 and SHK-1, as with the present modeled muscle cell. As indicated by the results it is seen that the action potentials demonstrate the all-or-none behavior shown by measurements reported by Liu *et al.* [14] and it is further seen that, though the values do not match completely, they resemble some of the features of the worm's own action potentials.

The upswing of the depolarization from our model

is approximately 71 ms, whereas Liu *et al.* report approximately 84 ms for the *slo-2* mutant [14]. This fast rise in potential can be attributed to the fast activation of the EGL-19 channel which is captured by the computational model. The amplitude obtained from our simulations is approximately 54.8 mV while previous findings for the actual worm are about 38 mV [14]. Our model also indicates the action potentials are 56.9 ms wide with the *slo-2* mutants being 28 ms [14]. The amplitude exhibited by our model's action potentials have a value of 54.8 mV. Those observed by Liu *et al.* were about 39 mV [14]. Despite some of the values differing it is demonstrated that the biological data is sufficient enough to produce action potentials in a computational model.

## 5 Conclusion

In this report we have demonstrated that enough information exists in the electrophysiological data of the *C. elegans* body wall muscle cell to produce action potentials. This, in itself, assures that a computational model of the body wall muscle cells is possible by considering only what we can observe from the actual living worm rather than relying on evolutionary fitting algorithms to assume what is thought to be missing. The discrepancies between the computational model and those observed by the *slo-2* mutant can be attributed to the lack of additional ion channels in the model. While the *slo-2* mutant does have EGL-19 and SHK-1 channels present in its genome, as with our model, there are other ion channels that affect the overall shape and timing of the action potentials. The model, as it stands, is still incomplete due to missing or inaccurate data that is sometimes conflicting in the literature.

As more data is reported, the model has the adaptability to grow and include this data the addition of more ion channels. In doing so, the model will gain accuracy when compared to biological reality. This model provides a foundation which enables a dynamic and flexible approach to the understanding of the *C. elegans* neuro-circuitry for locomotion, further expanding to more of the worm's behavior, ultimately including its entire nervous system.

## 6 Acknowledgments

This Material is based upon work supported by the National Science Foundation under Grant No. IIS-1350671. Consideration is also given to Steven Moreland for his insight on this report.



## References

- [1] Mathematica 9.0. Wolfram Research, Inc., 2012.
- [2] C.I. Bargmann. Neurobiology of *Caenorhabditis elegans* genome. *Science*, 282:2028–2033,, 1998.
- [3] J. Bryden and N. Cohen. Neural control of *Caenorhabditis elegans* forward locomotion: the role of sensory feedback. *Biological Cybernetics*, 98:339–351, 2008.
- [4] M. Driscoll and J. Kaplan. *Mechanotransduction, in C. Elegans*. Cold Spring Harbor Laboratory Press, 1997.
- [5] Gloria L. Fawcett, Celia M. Santi, Alice Butler, Thanawath Harris, Manuel Covarrubias, and Lawrence Salkoff. Mutant analysis of the Shal (Kv4) voltage-gated fast transient K<sup>+</sup> channel in *Caenorhabditis elegans*. *Journal of Biological Chemistry*, 281(41):30725–30735, 2006.
- [6] Shangbang Gao and Mei Zhen. Action potentials drive body wall muscle contractions in *Caenorhabditis elegans*. *Proceedings of the National Academy of Science*, 108(6):2557–2567, 2010.
- [7] A.L. Hodgkin and A.F. Huxley. A quantitative description of membrane current and its application to conduction and excitation in nerve. *Journal of Physiology*, 117(4):500–566, 1952.
- [8] Maëlle Jospin, Vincent Jacquemond, Marie-Christine Mariol, Laurent Ségalat, and Bruno Allard. The L-type voltage-dependent Ca<sup>2+</sup> channel EGL-19 controls body wall muscle function in *Caenorhabditis elegans*. *The Journal of Cell Biology*, 159(2):337–347, 2002.
- [9] Maëlle Jospin, Marie-Christine Mariol, Laurent Ségalat, and Bruno Allard. Characterization of K<sup>+</sup> currents using an *in situ* patch clamp technique in body wall muscle cells from *Caenorhabditis elegans*. *Journal of Physiology*, 544(2):373–384, 2002.
- [10] J. Karbowski and *et al.* Systems level circuit model of *C. elegans* undulatory locomotion: mathematical modeling and molecular genetics. *Journal of Computational Neuroscience*, 24:253–276, 2008.
- [11] Viviane Lainé, Christian Frøkær-Jensen, Harold Couchoux, and Maëlle Jospin. The  $\alpha 1$  subunit EGL-19, the  $\alpha 2/\delta$  subunit UNC-36, and the  $\beta$  subunit CCB-1 underlie voltage-dependent calcium currents in *Caenorhabditis elegans* striated muscle. *Journal of Biological Chemistry*, 286(42):36180–36187, 2011.
- [12] P. Liu, B. Chen, and Z-W. Wang. Gap junctions synchronize action potentials and Ca<sup>2+</sup> transients in *Caenorhabditis elegans* body wall muscle. *The Journal of Biological Chemistry*, 51(286):44285–44293, 2011.
- [13] P. Liu, B. Chen, and Z-W. Wang. Postsynaptic current bursts instruct action potential firing at a graded synapse. *Nature Communications*, 4(4):1911, 2013.
- [14] Ping Liu, Qian Ge, Bojun Chen, Lawrence Salkoff, Michael I. Kotlikoff, and Zhao-Wen Wang. Genetic dissection of ion currents underlying all-or-none action potentials in *C. elegans* body-wall muscle cells. *Journal of Physiology*, 589(1):101–117, 2011.
- [15] Qiang Liu, Bojun Chen, Eric Gaier, Jaya Joshi, and Zhao-Wen Wang. Low conductance gap junctions mediate specific electrical coupling in body-wall muscle cells of *Caenorhabditis elegans*. *Journal of Biological Chemistry*, 281(12):7881–7889, 2006.
- [16] MATLAB. *version 7.10.0 (R2010a)*. The MathWorks Inc., Natick, Massachusetts, 2010.
- [17] E. Neibur and P. Erdős. Theory of the locomotion of nematodes: Dynamics of undulatory progression on a surface. *Biophysics Journal*, 60:1132–1146, 1991.
- [18] C. M. Santi, A. Yuan, G. Fawcett, Z.-W. Wang, A. Butler, M.L. Nonet, A. Wei, P. Rojas, and L. Salkoff. Dissection of K<sup>+</sup> currents in *Caenorhabditis elegans* muscle cells by genetics and RNA interference. *Proceedings of the National Academy of Science*, 100(24):14391–14396, 2003.
- [19] K.A. Steger, B.B. Shitka, C. Thacker, T.P. Snutch, and L. Avery. The *C. elegans* T-type calcium channel CCA-1 boosts neuromuscular transmission. *Journal of Experimental Biology*, 208:2191–2203, 2005.
- [20] J.G. White and *et al.* The structure of the nervous system of the nematode *Caenorhabditis elegans*. *Philosophical Transactions of the Royal Society of London, Series B*, 314:1–340, 1986.
- [21] W.B. Wood. Introduction to *C. elegans* biology, in the nematode *Caenorhabditis elegans*. *Cold Spring Harbor Laboratory Press*, 1988.